

**Research Article**

## **SYNTHESIS AND CHARACTERIZATION OF ZnO NANO-PARTICLES**

**C. A. Omondi<sup>1</sup>, \*T. W. Sakwa<sup>1</sup>, Y. K. Ayodo<sup>1</sup> and K. M. Khanna<sup>2</sup>**

<sup>1</sup>*Department of Physics, Masinde Muliro University of Science and Technology, P.O. Box 190,  
Kakamega, Kenya*

<sup>2</sup>*Department of Physics, Chepkoilel University College, Moi University, P.O. Box 1125, Eldoret, Kenya*

*\*Author for Correspondence*

### **ABSTRACT**

The ZnO nanoparticles prepared by two different methods with the particle size of 320 nm and 559 nm exhibits XRD patterns that confirmed the presence of the required phase with diminutive traces of impurities. Unlike for ZnO-2, SEM micrographs of ZnO-1 sample showed that agglomeration took place. EDX of the ZnO-1 sample validated the presence of both Zn and O. DSC analysis of the ZnO-1 sample attests of the two endothermic reactions at temperatures 135 °C and 165 °C save for ZnO-2 sample which had only one peak at 150°C implying that only one endothermic reaction has taken place. The TGA analysis of the samples showed significant weight loss of about 5% and 10% at 135 °C and 165 °C temperatures respectively in case of ZnO-1, and a weight loss of about 10% at 150°C temperature for ZnO-2 sample.

**Key Words:** *Synthesis, Nanoparticles, Agglomeration*

### **INTRODUCTION**

Zinc oxide (ZnO) has featured as subject of thousands of research papers, dating back as early as 1935 (Bunn, 1935). Valued for its ultra violet absorbance, wide chemistry, piezoelectricity and luminescence at high temperatures, the study of ZnO relevant to the industry sector. It is found in paints, cosmetics, plastic and rubber manufacturing, electronics and pharmaceuticals, to name just a few (Look 2001). More recently however, ZnO entered the scientific spotlight for its semiconducting properties (Segawa *et al.*, 1997). Fuelled out of advances in growth technologies and the potential for ZnO to become a suitable substrate for GaN, the fabrication of high quality single crystals and epitaxial layers was achieved (Nause, 2005). Allowing for the realisation of ZnO-based photonic and optoelectronic devices, where, amongst other potential applications it stands with GaN as a prospective item for the next generation of light emitters for solid state lighting applications. With a wide band gap of 3.4 eV and a large exciton binding energy of 60 meV at room temperature, ZnO holds excellent promise for blue and ultra-violet optical devices (Look 2001). Although in the past GaN and GaN-based materials dominated this wavelength range, ZnO has advantages. One has to do with the larger exciton binding energy, which will allow for room temperature devices operating with higher efficiency and lower power threshold for lasing by optical pumping. The other advantage is the ability to grow high quality single crystal substrates with ease and effectively at low costs (Spaldin *et al.*, 2004; Coskun *et al.*, 2002; Kucheyev *et al.*, 2004). Other favourable aspects of ZnO include its broad chemistry leading to many opportunities for wet chemical etching, piezoelectric properties, radiation hardness and high ferromagnetic Curie temperature for spintronic applications (Pearson, 2004). Together, these properties make ZnO ideal for a variety of devices including blue and ultra-violet laser diodes and light emitting diodes. Despite the development of the field of semiconductors and the wide information base available for ZnO; as a semiconductor, little is actually known about this material. As with all wide band-gap semiconductors, ZnO has presented a number of hurdles to the scientific community which need to be understood and overcome before ZnO based devices can be commercially realised. The problems that initially hindered the realization of ZnO devices were solved (Segawa *et al.*, 1997). This includes mainly growth advances, which led the development of reproducible high quality epitaxial layers and single crystals.

Zinc oxide (ZnO) is of great interest as a suitable material for high temperature, high power electronic devices either as the active material or as a suitable substrate for epitaxial growth of group III-nitride

### **Research Article**

compound. UV photoconductivity of ZnO is governed by surface-related and bulk-related processes (Spaldin 2004). The surface-related process is primarily governed by the adsorption and desorption of the chemisorbed oxygen at the surface of the ZnO, which is exploited for gas sensing applications. This process becomes prominent in nanocrystalline films, where the surface area is large. In the bulk-related process, oxygen molecules in the grain boundaries contribute to photoconductivity. The bulk-related process is however considered to be faster in comparison to the surface-related process. Pearton SJ (2004). For UV-detection, the fast component, due to the generation of photo carriers and their radiative and non-radiative recombination through local centres, is of greater importance. Inherent defect centres, such as oxygen vacancies and zinc interstitials are believed to be responsible for visible photoluminescence in ZnO (Look *et al.*, 2004). It has been shown that recombination centers responsible for the orange band were the centers of photosensitivity. Defects in ZnO strongly depend on the preparation and annealing conditions which in turn affect the photoconduction properties (Zhang *et al.*, 2001; Van de Walle, 2000). There have been studies on the effect of annealing under different conditions on the defect-related emission of ZnO thin films and nanostructures. The air-annealed ZnO films are preferable for photodetector applications due to the lower dark current. The large concentration of defects in the ZnO nanostructures prepared at low temperatures can be controlled by annealing in oxygen at different temperatures. It is therefore important to carry out a study of the effect of annealing temperature on the photoluminescence as well as the photoconduction properties of ZnO nanostructures. In this communication, we report the effect of annealing in an oxygen atmosphere on the photoluminescence and photoconducting properties of thin films of colloidal ZnO nanoparticles.

## **MATERIALS AND METHODS**

### ***Synthesis of ZnO-1***

Zinc Oxide (ZnO) nanoparticles were prepared by wet chemical method using zinc nitrate and sodium hydroxides precursors with soluble starch as stabilizing agent. Different concentrations of soluble starch (0.1%), were dissolved in 500 ml of distilled water by using microwave oven. Zinc nitrate, 14.874g (0.1 mol), was added in the above solution. Then the solution was kept under constant stirring using magnetic stirrer to completely dissolve the zinc nitrate for one hour. After complete dissolution of zinc nitrate, 0.2 mol of sodium hydroxide solution was added under constant stirring, drop by drop touching the walls of the vessel. The reaction was allowed to proceed for 2 h after complete addition of sodium hydroxide. After the completion of reaction, the solution was allowed to settle for overnight and the supernatant solution was then discarded carefully. The remaining solution was centrifuged at 10,000'g for 10min. Thus obtained nanoparticles were washed three times using distilled water. Washing was carried out to remove the by-products and the excessive starch that were bound with the nanoparticles. After washing, the nanoparticles were dried at 80°C overnight. While drying, complete conversion of Zn (OH)<sub>2</sub> into ZnO took place.

### ***Synthesis of ZnO-2***

Zinc oxide was prepared from Zinc nitrate solution after neutralizing with NaOH to pH values of 12. When the reactions were complete, the solid and solution phases were separated by centrifugation and the solids washed free of salts with de-ionized water three times and with ethanol two times. Then a white color powder was calcinated at 80 °C and then grinded for uniformities of the powder. The dry synthetic powders were weighed and the percentage yields were determined from the expected total amount of ZnO based on the solution concentration, the volume and the amount that was actually crystallized.

The nanoparticles were analysed by means of XRD measurements whose patterns were recorded from 20° to 90° with a PAN-analytical system diffractometer (Model: DY-1656) using Cu K $\alpha$  ( $\lambda=1.542\text{\AA}$ ) with an accelerating voltage of 40 KV. Data was collected on a counting rate of 1°/min. The K $\alpha$  doublets were well resolved. From XRD, the crystallite size can be found out by using the scherrer's formula. The composition of elements like Zn and O, are confirmed by EDX.

**Research Article**

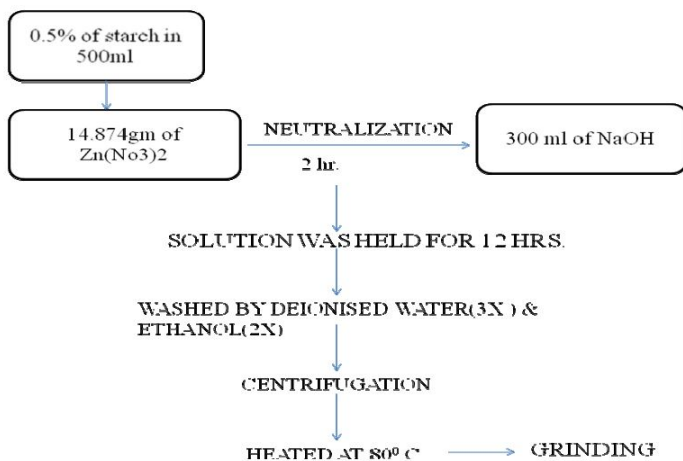


**Figure 1: Schematic diagram of synthesis of ZnO-1 sample**

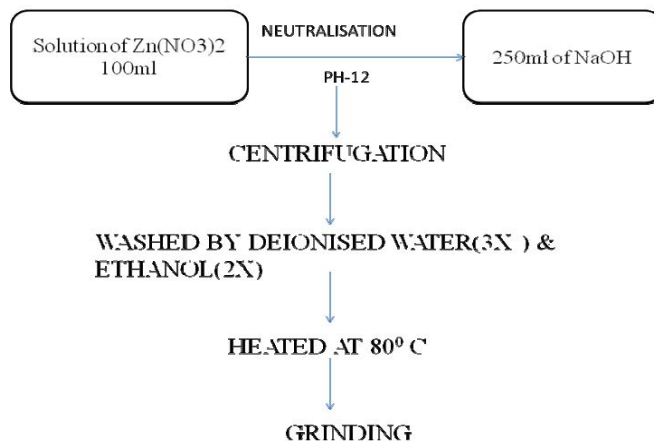


**Figure 2: Schematic diagram of synthesis of ZnO-2 sample**

The ZnO nanoparticles were investigated by both optical microscope and electron scanning microscope (SEM) operating at magnification of X5000, 15kV. The SEM analysis of the ZnO-1 and ZnO-2 samples prepared from two different methods were done by SEM (JEOL-JSM 5800). The microscopic view of the ZnO in powder and in the dispersed form were taken by optical microscope with a magnification of 40X as shown in figures 7 and 8.

Particle size of the milled powder was measured by Malvern particle size analyzer (Model Micro-P, range 0.05-550 micron). Firstly, the liquid dispersant containing 500ml of distilled water and 25 ml of sodium hexa metaphosphate was kept in the sample holder. Then the instrument was run keeping ultrasonic displacement at 10.00 micron and pump speed 1800 rpm. A pinch of powders was added to the liquid dispersant so that the obscuration value varies between 10 to 30% and the residual below 1%. The Differential Scanning Calorimetric analysis of the ZnO samples was done by heat-flux calorimeter 2920 DSC (Thermal Analysis Instruments), both sample showing different reactions happening. TGA analysis of the samples ZnO-1 and ZnO-2 were done by an instrument with a heating rate of 10 C/min.

## Research Article

### RESULTS AND DISCUSSION

#### X-ray Diffraction (XRD)

X-ray diffraction measurements for bulk ZnO and nano ZnO as exhibited in the figures 3 and 4 of the diffractograms of ZnO-1 and ZnO-2 samples depicts highest peaks at same angle of  $36.50^\circ$  implying that the samples were same.

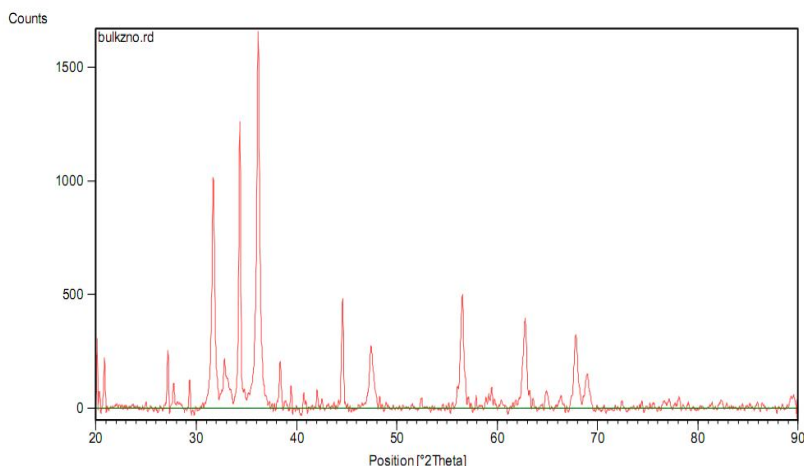


Figure 3: XRD of ZnO-1

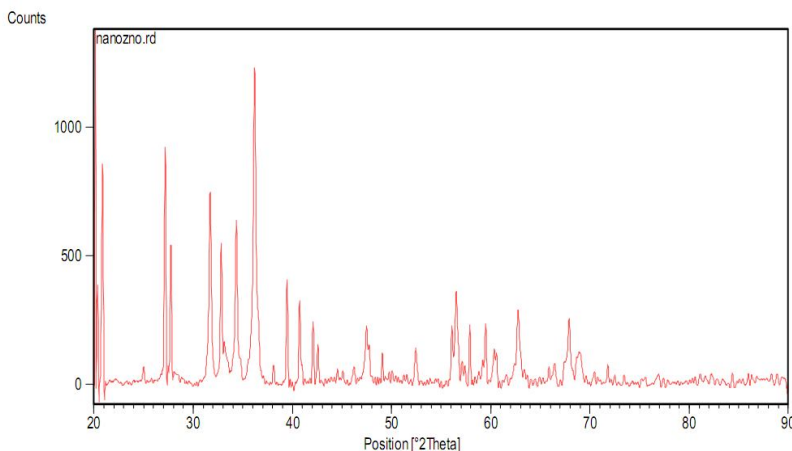


Figure 4: XRD of ZnO-2

#### SEM Results

The micrographs shown in figure 5 reveals a network formation of the ZnO-1 which clearly indicates that agglomeration took place too. Similarly, in figure 6, a major aggregation of the sample ZnO-2 particles happened. It is not possible to predict the exact size of the individual particle except by TEM analysis. From the micrograph, it can be concluded that the particles are irregular in shape.

The microscopic view was taken by optical microscope with a magnification of 40X. At first the microscopic view of the powder was taken (see figure 7) before the powder of ZnO-2 sample was dispersed in water and the microscopic view taken again as shown in figure 8.

#### EDX Results

The EDX of the ZnO-1 sample done by the SEM (JEOL-JSM 5800) machine confirmed the presence of the required phase of both Zinc (Zn) and Oxygen(O). However, the presence of Mg. and Si as observed

**Research Article**

in figures 9 is due to the components in the substrate over which the sample was held to do the SEM characterization.

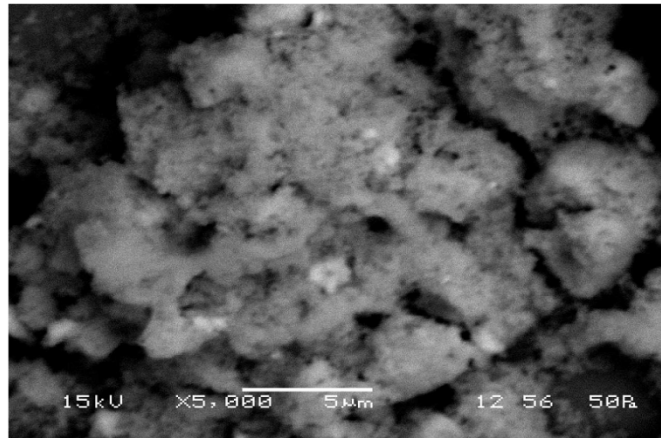


**Figure 5: SEM of ZnO-1**

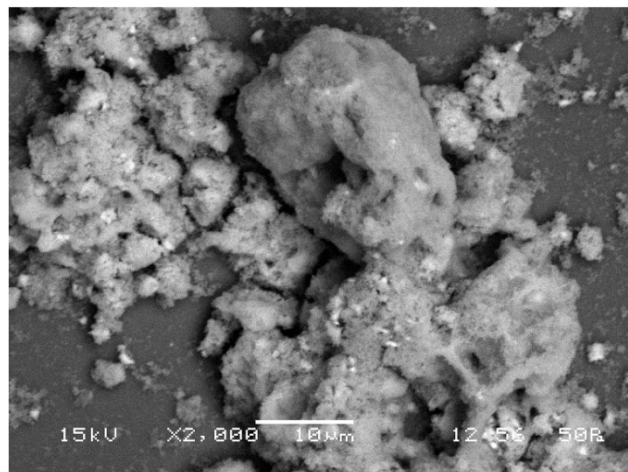


**Figure 6: SEM of ZnO-2.**

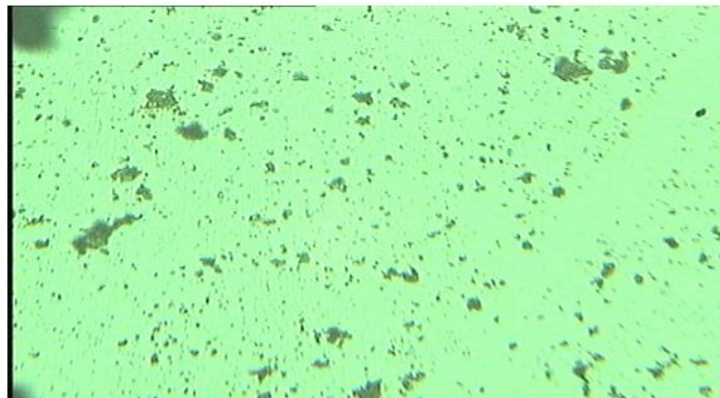


**Figure 7: Microscopic view of ZnO-2 in powder form**

**Research Article**

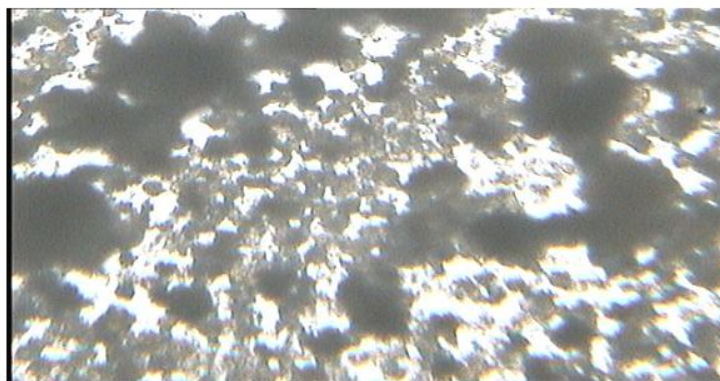


**Figure 8:** Microscopic view of ZnO-2 in dispersed form

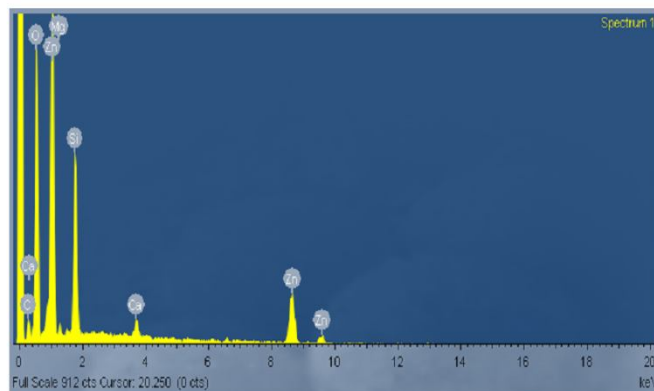


**Figure 9:** EDX of ZnO-1

**Particle Size Analyzer.**

Figures 10 and 11 shows the particle sizes of ZnO-1 and ZnO-2 samples which, after the analysis, were found to be 320 nm and 559 nm respectively.

**DSC Characterization**

Differential scanning calorimeters measured the amount of heat absorbed or released during such transitions. Positions of all these peaks depend on heating rate. Increasing the heating rate causes every peak to shift towards higher temperatures, with the first two endothermic peaks merged into one broad one. This is due to activation energy involved in such transition. In the ZnO-1 sample there are two peaks at around 135<sup>o</sup>C and 165<sup>o</sup>C. Both are endothermic reactions which is due to change of phases at those temperatures. Similarly in the ZnO-2 sample there is only one peak at 150<sup>o</sup>C.

**Thermo Gravimetric Analysis**

The TGA of the sample ZnO-1 showed a continues weight loss up to 500<sup>o</sup>C, after which there was no significant loss of heat. At 135<sup>o</sup>C and 165<sup>o</sup> C, a sharp weight loss was noticed as depicted in figure 13. Similarly, the TGA of ZnO-2 showed only one sharp down fall at 150<sup>o</sup> C, which was a significant weight loss; though there was a continues weight loss up to 700<sup>o</sup>C.

**Research Article**

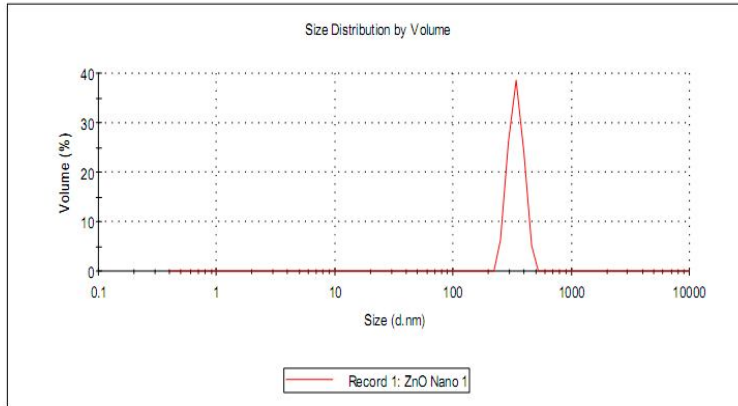


**Figure 10: Particle size of ZnO-1**

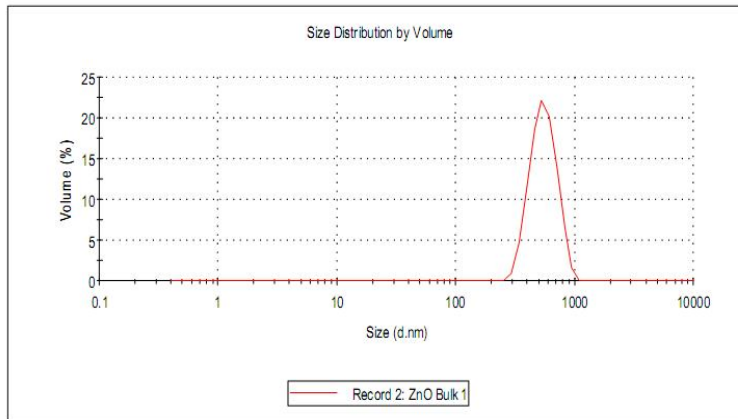


**Figure 11: Particle size of the ZnO-2**

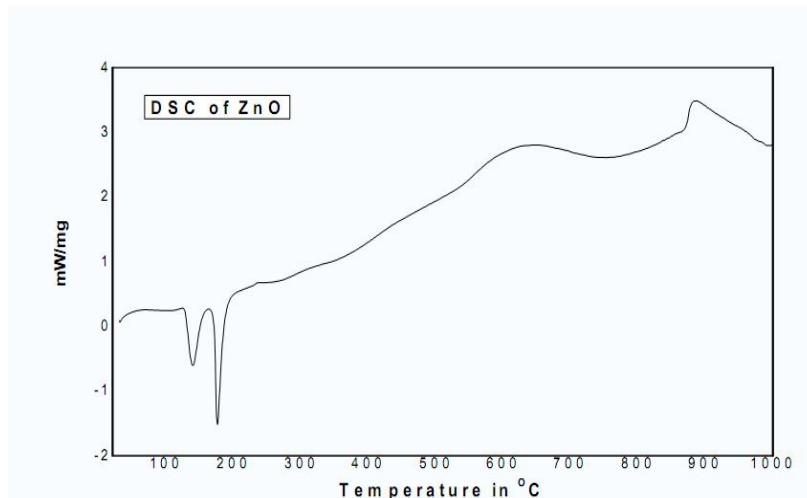


**Figure 12: DSC analysis of ZnO-1**

**Research Article**

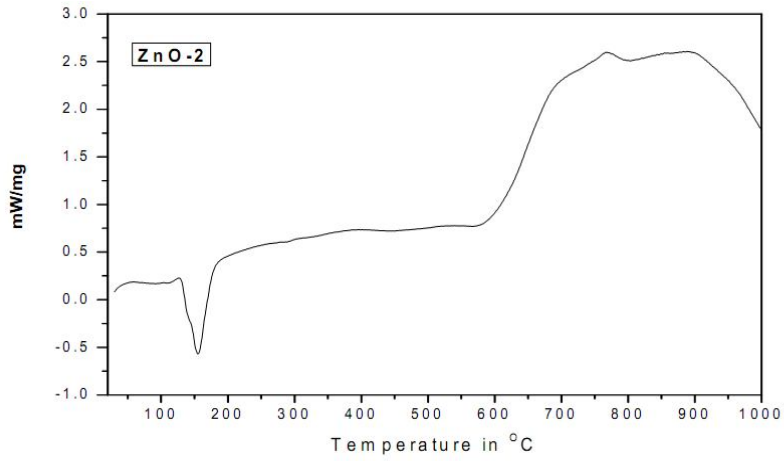


**Figure13: DSC analysis of ZnO-2**

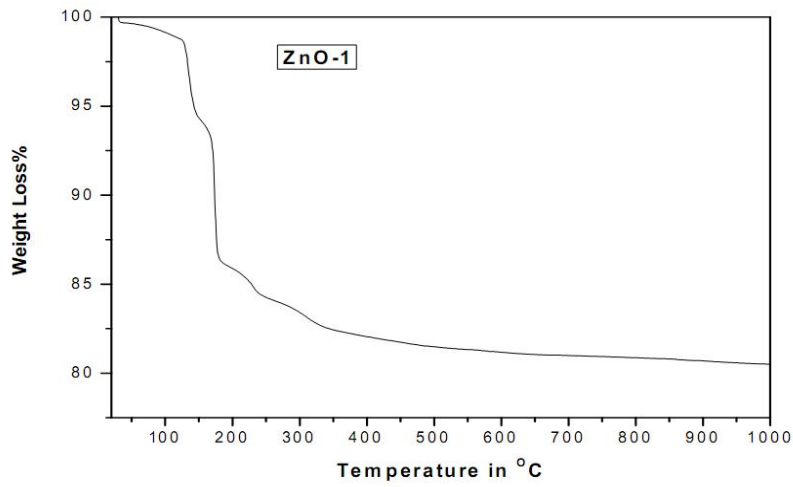


**Figure14: TGA analysis of ZnO-1**

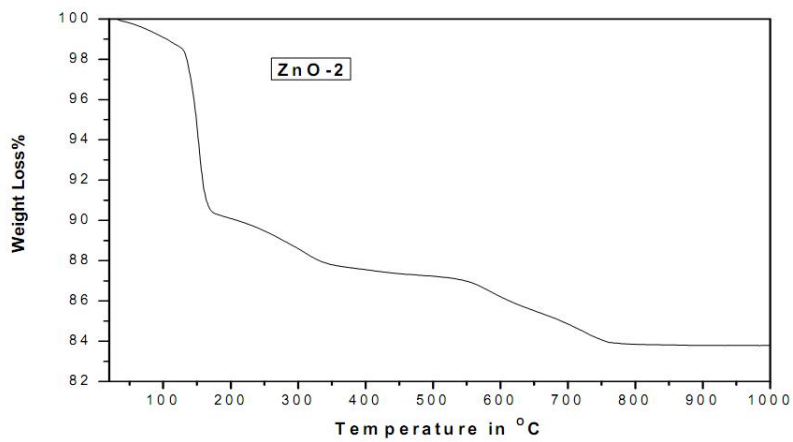


**Figure 15: TGA analysis of ZnO-2**

## **Research Article**

### **Conclusion**

The XRD of the ZnO nanoparticles samples revealed that the required phase had some impurities. The particle size analysis was supported by the XRD Scherer's formula. Unlike in ZnO-2, the SEM of the ZnO-1 sample showed that agglomeration took place. The particle size is irregular prepared from both the methods. Both Zn and O were present along with Mg and Si when the ZnO-1 sample was held by a glass substrate for characterization. DSC of the ZnO-1 ensures that two endothermic reactions have been taken place at temperature around 135<sup>0</sup>C and 165<sup>0</sup>C. Endothermic reactions are due to change of phases at that temperature. However, in the ZnO-2 sample there was only one peak at 150<sup>0</sup>C. TGA analysis of both the sample supports the results coming out from DSC analysis that the weight loss were seen at 135<sup>0</sup> C and 165<sup>0</sup> C in the ZnO-1 sample of about 5% and 10% respectively and in case of ZnO-2 sample, the weight loss was about 10% at 150<sup>0</sup>C. Different characteristics of the samples could be as a result of variations in sample sizes.

### **ACKNOWLEDGEMENTS**

We would like to express sincere gratitude to the head of the department of electronic science of the Fergusson college, Prof. J.V Khedkar and vice principals (Dr. N.M Kulkani and Prof. A.B. Bhide) for allowing us to access their research facilities. We also appreciate Masinde Muliro University of Science and Technology who gave me a platform to share our talents and skills as their dedicated employees.

### **REFERENCES**

- Bunn CW (1935).** The lattice-dimensions of zinc oxide. *Proceedings of the Physical Society London* **47**(5) 835.
- Look DC (2001).** Recent advances in ZnO materials and devices. *Journal of Material Science and Engineering B* **80**(1-3) 383-387.
- Segawa Y, Ohtomo A, Kawasaki M, Koinuma H, Tang HZK, Yu P and Wong GKL (1997).** Growth of ZnO thin films by laser-MBE: Lasing of excitons at room temperature. *Physica Status Solidi B-Basic Research* **202**(2) 669-672.
- Nause JE (2005).** Fluorescent substrate offers route to phosphor-free LEDs. *Components of Semiconductor* **11**(29).
- Coskun C, Look DC, Farlow GC and Sizelove JR (2004).** Radiation hardness of ZnO at low temperatures. *Semiconductor Science and Technology* **19**(6) 752.
- Kucheyev SO, Williams JS and Jagadish C (2004).** Ion-beam-defect processes in group-III nitrides and ZnO. *Vacuum* **73** 93-104.
- Spaldin NA (2004).** Search for Ferromagnetism in transition-metal-doped piezoelectric ZnO. *Physical Review B* **69** 125 201.
- Pearson SJ, Norton DP, Ip K, Heo Y and Steiner T (2004).** Recent advances in processing of ZnO. *Journal of Vacuum Science & Technology B* **22**(3) 932.
- Look DC and Claflin B (2004).** P-type doping and devices based on ZnO. *Physica Status Solidi B* **241** (3) 624-630.
- Look DC, Claflin B, Alivov YI and Park SJ (2004).** The future of ZnO light emitters. *Physica Status Solidi A* **201**(10) 2203-2212.
- Zhang SB, Wei SH and Zunger A (2001).** Intrinsic n-type versus p-type doping asymmetry and the defect physics of ZnO. *Physical Review B* **63** 075 205.
- Look DC and Claflin B(2004).** P-type doping and devices based on ZnO. *Physica Status Solidi (B)* **241**(3) 624–630
- Look DC, Claflin B, Alivov YI and Park SJ (2004).** The future of ZnO light emitters. *Physica Status Solidi A* 201(10) 2203-2212.

**Research Article**

**Zhang SB, Wei SH, Zunger A , 2001.** Intrinsic n-Type Versus p-Type Doping Asymmetry and the Defect Physics of ZnO. *Physical Review B* **63** 075-205

**Van de Walle CG (2000).** Hydrogen as a cause of doping in ZnO. *Physical Review letter* **85**(5) 1012-5.